

BEST sensitivity to O(1) eV sterile neutrinoVladislav Barinov,^{1,2,*} Vladimir Gavrin,^{1,†} Dmitry Gorbunov,^{1,3,‡} and Tatiana Ibragimova^{1,§}¹*Institute for Nuclear Research of the Russian Academy of Sciences, Moscow 117312, Russia*²*Physics Department, Moscow State University, Vorobievsky Gory, Moscow 119991, Russia*³*Moscow Institute of Physics and Technology, Dolgoprudny 141700, Russia*

(Received 17 February 2016; published 8 April 2016)

Numerous anomalous results in neutrino oscillation experiments can be attributed to the interference of an ~ 1 eV sterile neutrino. The Baksan Experiment on Sterile Transitions (BEST), specially designed to fully explore the Gallium anomaly, starts next year. We investigate the sensitivity of BEST in search of a sterile neutrino mixed with an electron neutrino. Then, performing the combined analysis of all the Gallium experiments (SAGE, GALLEX, BEST), we find the region in the model parameter space (sterile neutrino mass and mixing angle) which will be excluded if BEST agrees with no sterile neutrino hypothesis. For the opposite case, if BEST observes the signal as it follows from the sterile neutrino explanation of the Gallium (SAGE and GALLEX) anomaly, we show how BEST will improve upon the present estimates of the model parameters.

DOI: 10.1103/PhysRevD.93.073002

I. INTRODUCTION

Neutrino oscillations¹ provide the only direct irrefutable evidence for incompleteness of the Standard Model of particle physics (SM). Moreover, while most issues of the neutrino experiments can be properly addressed by making at least two out of three SM neutrinos massive, there are several *anomalous* results which are definitely beyond the grasp of this simple extension.

The results of experiments LSND [1,2], MiniBooNE [3,4], SAGE [5,6], GALLEX [7], and analysis of measured reactor antineutrinos [8,9] show an *anomalous change of neutrino fluxes*. If attributed to oscillations, it requires much bigger values of a neutrino squared mass difference, $\Delta m_{\text{anom}}^2 \approx 1 \text{ eV}^2$, as compared to the already known values of the two mass squared differences (so called solar, $\Delta m_{\text{sol}}^2 \approx 7.5 \times 10^{-5} \text{ eV}^2$ and atmospheric, $\Delta m_{\text{atm}}^2 \approx 2.5 \times 10^{-3} \text{ eV}^2$ [10]) sufficient to explain the results of the great majority of neutrino oscillation experiments. The hierarchy between the two mass differences, $\Delta m_{\text{sol}}^2 \ll \Delta m_{\text{atm}}^2$, can be described by three neutrino eigenstates and hence, is consistent with the three neutrino pattern. The third mass difference making the pronounced hierarchy $\Delta m_{\text{sol}}^2 \ll \Delta m_{\text{atm}}^2 \ll \Delta m_{\text{anom}}^2$ asks for (at least) one more neutrino eigenstate that the SM does not have. A hunt for the new light neutrino species is the main task of many developing projects [11].

The anomalies naturally form two classes. There are anomalous appearances (excesses of signal events) and anomalous disappearances (lacks of signal events). An anomalous disappearance of neutrinos can point to oscillations into the (hypothetical) fourth light neutrino state, a singlet with respect to the SM gauge group, and hence, called *sterile*, while the SM neutrinos are dubbed *active*. In particular, observed by experiments SAGE [12] and GALLEX [7] lack of electron neutrinos from artificial radioactive neutrino sources can be explained by oscillations into sterile neutrinos, which obviously escape detection. Then electron neutrino flux measured at a distance r from the source is proportional to the electron neutrino *survival probability* (against transition into the sterile state). For the artificial sources under discussion, the neutrino flux is quasimonochromatic. The survival probability for a neutrino of an energy E_ν is determined in the two-neutrino effective oscillating system through the sterile-active mixing angle θ and the squared mass difference Δm^2 (saturated mostly by the sterile neutrino squared mass) as follows, see, e.g., [13],

$$P(E_\nu, r) = 1 - \sin^2 2\theta \sin^2 \left(1.27 \times \frac{\Delta m^2 [\text{eV}^2] r [\text{m}]}{E_\nu [\text{MeV}]} \right). \quad (1)$$

The joint analysis [14] of the four gallium anomalous results (two per each experiment) reveals the anomaly—disappearance of electron neutrinos—at the statistical level of 2–3 standard deviations. Within the hypothesis of oscillations into the sterile neutrino, the best fit of model parameters entering the survival probability (1) have typical values in the region [15]

*barinov.vvl@gmail.com

†gavrin@inr.ru

‡gorby@ms2.inr.ac.ru

§tvi@inr.ru

¹There are antineutrino oscillations as well, but in the general discussion, we do not distinguish the two cases.

$$\Delta m^2 \sim 2 \text{ eV}^2, \quad \sin^2 2\theta \sim 0.3\text{--}0.5. \quad (2)$$

The new gallium experiment BEST [11,16,17] in Baksan neutrino observatory was proposed to thoroughly explore the gallium anomaly. It is a short-baseline experiment utilizing the artificial compact ^{51}Cr source of almost monochromatic electron neutrinos to be measured at effectively two distances of $\sim 0.4 \text{ m}$ and $\sim 0.8 \text{ m}$ from the source. After accurate measurement and detailed analysis of the neutrino-gallium cross section [18–20], it has been recently approved, see Refs. [21–25] for description of the passed and present research and development stages. It will start supposedly next year with the production of an artificial 3 MCi radioactive ^{51}Cr source of electron neutrinos. In this paper, we refine the preliminary estimates [11] of the BEST sensitivity to the sterile neutrino parameters and its prospects in exploring the gallium anomaly.

The paper is organized as follows. Section II contains brief descriptions of the main idea of the experiment, the artificial source, detecting technique, data processing, registration efficiency, and final accuracy in the measurement of the electron neutrino flux. We discuss the anomalous results of the gallium experiments in Sec. III and present the region in the sterile neutrino model parameter space (Δm^2 , $\sin^2 2\theta$) favored by the gallium anomaly. In Sec. IV, we outline the regions to be excluded by BEST, if its result is consistent with no oscillation hypothesis, and the regions to be excluded by the joint analysis of all the gallium experiments. Likewise, we consider the possibility that the BEST future result is consistent with predictions of the sterile neutrino model with parameters tuned at the best-fit to the gallium anomaly; we outline the favored by BEST region in this case and present the region chosen by the joint analysis of all the Gallium experiments. We summarize in Sec. V.

II. DESCRIPTION OF THE EXPERIMENT: LAYOUT, OPERATION, AND DATA ANALYSIS

BEST is a short-baseline neutrino oscillation experiment. The size is determined from Eq. (1) by the best-fit values (2), which for MeV-scale neutrino energy implies a 1 m-scale oscillation length. The artificial radioactive source of 3 MCi is made of ^{51}Cr , which decays emitting quasimonochromatic neutrinos of energies $E_{1a} = 0.747 \text{ MeV}$ (dominant mode), $E_{1b} = 0.752 \text{ MeV}$, $E_{2a} = 0.427 \text{ MeV}$, and $E_{2b} = 0.432 \text{ MeV}$. The source intensity is measured with at least 0.5% accuracy by making use of the methods presented in Refs. [26–28].

The source is a solid homogeneous cylinder with a diameter of about 9 cm and a height of about 10 cm. It is placed in the center of a sphere of radius $r_1^{\text{BEST}} = 0.66 \text{ m}$ filled with the homogeneous liquid gallium ^{71}Ga . The sphere is inside the cylindrical vessel of radius $r_2^{\text{BEST}} = 1.096 \text{ m}$ and height $2 \times r_2^{\text{BEST}}$ also filled with the homogeneous liquid gallium, see Fig. 1. The allocation for the artificial

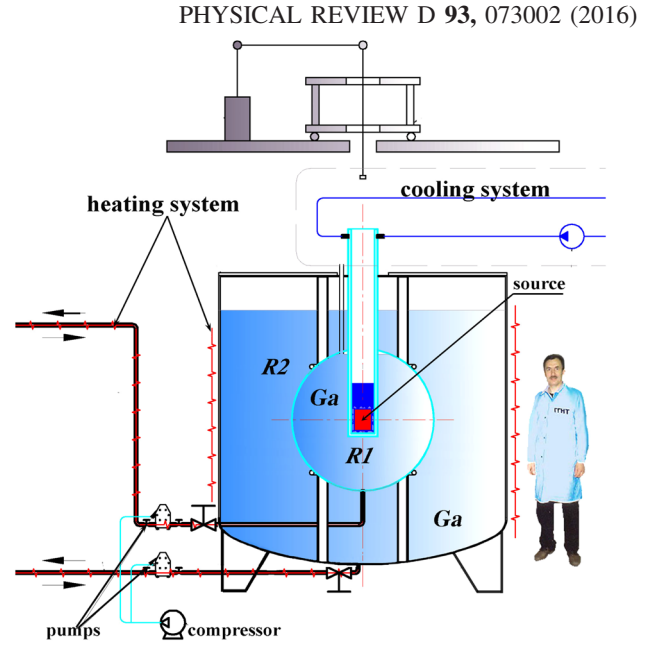


FIG. 1. BEST layout, vessel sizes are $R1 = r_1^{\text{BEST}}$, $R2 = r_2^{\text{BEST}}$.

source central part of the construction can be approximated² as a spherical region of radius $r_c^{\text{BEST}} = 10.5 \text{ cm}$. Only this part is free of gallium. The electron neutrinos can be captured by ^{71}Ga nuclei, which turn into ^{71}Ge . This germanium isotope decays solely by electron capture to the ground state of ^{71}Ga with a half-life of 11.43 d. Without oscillations to the sterile neutrinos, at the beginning of irradiation, the mean production rate of ^{71}Ge in each zone is 65 atoms per day. After an exposure period, the ^{71}Ge atoms produced by neutrino capture are extracted from the gallium and counted separately for each vessel with mostly the same technique [21] as used for the SAGE experiment. The lifetime of ^{51}Cr is 27.7 d, and several subsequent extractions are planned. A Monte Carlo simulation of the entire experiment—10 extractions each with a 9-day exposure—which uses typical values of extraction efficiency, counter efficiency, counter background rates, and includes the known solar neutrino rate, indicates that the rate in each zone can be measured with a statistical uncertainty of about 3.7%. An expected total systematic uncertainty is about 2.7%. The combined fit to the 10 extractions enables measurement of the electron neutrino flux keeping it under control in each vessel with an accuracy better than 5% [11,25].

III. GALLIUM ANOMALY

We start with the analysis of anomalous results, observed in SAGE and GALLEX, to find the region in sterile

²The use of the effective geometry changes the neutrino count rate by less than 2% [11], which is a negligible impact on our estimates of the BEST sensitivity.

neutrino parameter space $(\Delta m^2, \sin^2 2\theta)$ favored by the explanation of the anomaly as oscillations into the sterile neutrinos.

In SAGE, the artificial sources have been placed in the center of a spherical vessel, which for our purposes may be approximated as a sphere of radius $r^{\text{SAGE}} = 72.6$ cm with a central part of radius $r_c^{\text{SAGE}} = 25.3$ cm free of gallium and allocated for the source. The artificial sources were of the cylindrical form with a height of 15 cm and a diameter of 9.5 cm [5]. It can be approximated as a sphere of radius $r_s^{\text{SAGE}} = 6.3$ cm. In the first experiment, the ^{51}Cr source was used. It provided the same neutrino spectrum as in case of BEST, which is effectively two-peak with energy lines at $E_1 = 0.75$ MeV (dominant peak) and $E_2 = 0.43$ MeV. In the second experiment, the ^{37}Ar source was used. The dominant neutrino mode is at $E_1 = 0.811$ MeV, the subdominant is very close, $E_2 = 0.813$ MeV, so the source is monochromatic with a high accuracy.

Neutrino flux at the distance r from the source is proportional to the survival probability (1). The rate of induced transitions $^{71}\text{Ga} \rightarrow ^{71}\text{Ge}$ is also proportional to the gallium density, which was uniform, and to the neutrino capture cross section, $\sigma_{\text{Ga}}(E)$, which is different for different neutrino energies and has been recently refined [18–20]. The contribution of each neutrino line to the number of the transition is weighted with the intensity of the line and neutrino capture cross section $\sigma_{\text{Ga}}(E_i)$, $i = 1, 2$. Finally, for the ratio of the signal expected within the sterile neutrino hypothesis and the signal expected without sterile neutrino, we obtain

$$R^{\text{th}} = \frac{1}{\Delta L} \int_{r_1}^{r_2} dr [P(E_1, |\vec{r} - \delta\vec{r}|) f_1 + P(E_2, |\vec{r} - \delta\vec{r}|) f_2], \quad (3)$$

where the relative contributions of the two lines in the ^{51}Cr source are $f_1 = 0.96$, $f_2 = 0.04$, the integration goes between the radius of the central part $r_1 = r_c^{\text{SAGE}}$ and the vessel radius $r_2 = r^{\text{SAGE}}$, the normalizing effective length is $\Delta L = r_2 - r_1$; the results are further averaged over the artificial source of a finite size (variable $\delta\vec{r}$) adopting the spherical approximation with radius r_s^{SAGE} .

Likewise, this formula can be applied to describe the results of the SAGE experiment with ^{37}Ar source.

The two measurements in GALLEX experiment [29] have been performed with ^{51}Cr radioactive sources. In each case, the radioactive source can be approximated by a homogeneous sphere of radius $r_s^{\text{GALLEX}} \approx 0.4$ m. The source was placed in the center of the vessel, which for our purposes can be approximated as a sphere of radius $r^{\text{GALLEX}} \approx 2.5$ m, the radius of the central part with the source is $r_c^{\text{GALLEX}} \approx 0.45$ m. To describe the expected ratio of the signals with sterile neutrino and without sterile neutrino, one can use the same formula (3) with the same

values of E_i and f_i , as those adopted for the SAGE with ^{51}Cr source, and $r_1 = r_c^{\text{GALLEX}}$, $r_2 = r^{\text{GALLEX}}$.

The anomalous results read [14]

$$\begin{aligned} R_{\text{SAGE}}^{\text{obs}}(^{51}\text{Cr}) &= 0.95 \pm 0.12, \\ R_{\text{SAGE}}^{\text{obs}}(^{37}\text{Ar}) &= 0.79 \pm 0.10, \\ R_{\text{GALLEX}}^{\text{obs}}(^{51}\text{Cr}) &= 0.953 \pm 0.11, \\ R_{\text{GALLEX}}^{\text{obs}}(^{51}\text{Cr}) &= 0.812 \pm 0.11. \end{aligned} \quad (4)$$

The best fit values of the sterile neutrino model parameters $(\Delta m^2, \sin^2 2\theta)$ entering the theoretical expectations (3) through the survival probability (1), can be obtained by minimizing the χ^2 statistics defined as the following sum over all of the four experiments

$$\chi^2 = \sum_{i=1}^4 \frac{(R_i^{\text{obs}} - R_i^{\text{th}}(\Delta m^2, \sin^2 2\theta))^2}{\sigma_i^2}, \quad (5)$$

where σ_i stand for corresponding uncertainties in the measured values (4).

We find for the best-fit value

$$\Delta m^2 \approx 2.3 \text{ eV}^2, \quad \sin^2 2\theta \approx 0.24, \quad (6)$$

which we exploit below as a refined version of the estimate (2). In Fig. 2, we present the contours outlining the regions consistent with the sterile neutrino explanation of the anomaly at 1σ , 2σ , and 3σ confidence levels. The contours refer to the corresponding marginal values of $\chi^2 = \chi^2_{\text{min}} + \Delta\chi^2$ for $\Delta\chi^2$ with two free parameters: $\Delta\chi^2 = 2.30, 6.18, 11.83$, respectively [10]; the oscillation parameters

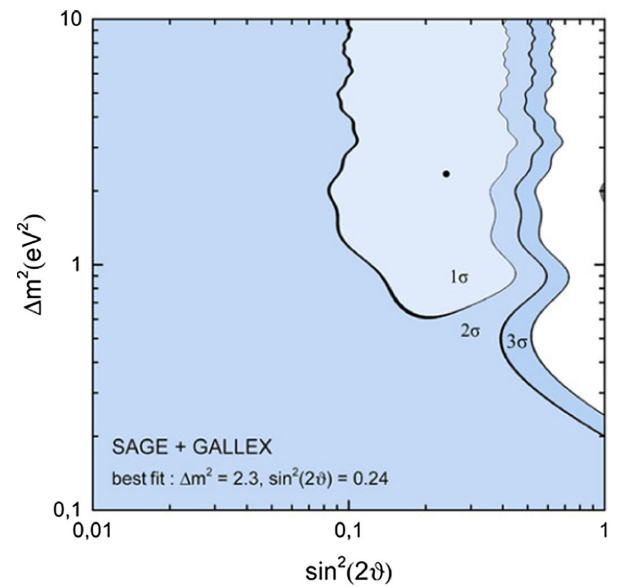


FIG. 2. Regions, obtained from the combined analysis of the results of the four radioactive source experiments by SAGE and GALLEX. The best fit value is (6).

Δm^2 , $\sin^2 2\theta$ are adopted in the minimized χ^2 function for the four gallium radioactive source experiments. As one observes from Fig. 2, the lines of constant χ^2 forms a rather shallow profile, so the best-fit value (6) is not actually indicative: the 1σ region is quite broad, $\Delta m^2 \gtrsim 0.7 \text{ eV}^2$, $0.1 \lesssim \sin^2 2\theta \lesssim 0.4$. It is in agreement, of course, with the statement [14] that the statistical significance of the observed anomaly is not high at the level of 2–3 σ , as we mentioned in the Introduction.

IV. SENSITIVITY CONTOURS

As noticed in Sec. II, the technique used in BEST allows us to measure the ratio R in each vessel with an accuracy of about $\sigma_{\text{BEST}} = 0.05 \times R$. The presence of two vessels enables performing two independent experiments at the same time. The predictions for the expected ratios are given by the same formula (3) with $r_1 = r_c^{\text{BEST}}$ and $r_2 = r_1^{\text{BEST}}$ for experiment one and $r_1 = r_1^{\text{BEST}}$ and $r_2 = r_2^{\text{BEST}}$ for experiment two.

Further, we treat the would-be measured at BEST ratio R_m as a random Gaussian variable with a central value R_c and standard deviation $\sigma_{\text{BEST}} = 0.05 \times R_c$, so that R_m is distributed as

$$D_{R_c, \sigma_{\text{BEST}}}(R_m) = \frac{1}{\sqrt{2\pi}\sigma_{\text{BEST}}} \exp\left(-\frac{(R_m - R_c)^2}{2\sigma_{\text{BEST}}^2}\right). \quad (7)$$

For each value of R_m , the corresponding model parameters are determined by the maximization of the likelihood function

$$\mathcal{L}_{\sigma_{\text{BEST}}}(\Delta m^2, \sin^2 2\theta; R_m) \propto \exp\left(-\frac{(R_m - R^{\text{th}}(\Delta m^2, \sin^2 2\theta))^2}{2\sigma_{\text{BEST}}^2}\right). \quad (8)$$

Suppose, that the BEST results are consistent with a particular theory prediction R_c . Then within the Bayesian approach, the favored value of the sterile neutrino parameters are determined from (8) marginalized over R_m with Gaussian prior (7), which gives

$$\int dR_m \mathcal{L}_{\sigma_{\text{BEST}}}(\Delta m^2, \sin^2 2\theta; R_m) D_{R_c, \sigma_{\text{BEST}}}(R_m) = \mathcal{L}_{\sqrt{2}\sigma_{\text{BEST}}}(\Delta m^2, \sin^2 2\theta; R_c).$$

Thus, the favored model parameters are distributed as (8) with the following replacement $R_m \rightarrow R_c$ and $\sigma_{\text{BEST}} \rightarrow \sqrt{2}\sigma_{\text{BEST}}$.

Then the BEST sensitivity can be obtained using the same χ^2 expression (5) with $R_i^{\text{obs}} = R_c$ and $\sigma_i = \sqrt{2}\sigma_{\text{BEST}}$. To illustrate this formula in Fig. 3, we present the plots with exclusion regions for two cases: (top panel) BEST observations are fully consistent with only three neutrino states, i.e., $R_c = 1$ for each vessel; (bottom panel) BEST

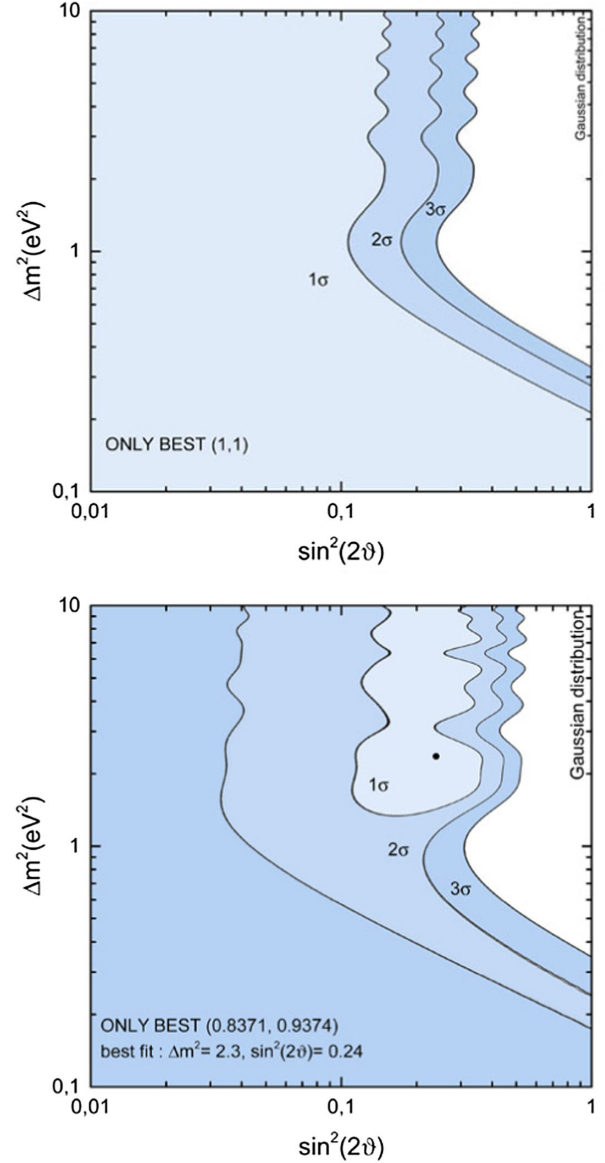


FIG. 3. Regions, favored by the BEST experiment in cases: (upper panel) it finds no anomaly, (lower panel) it confirms the gallium anomaly; see the main text for details.

observations are fully consistent with the best-fit oscillation parameters (6) from the sterile neutrino explanation of the gallium anomaly, which for the BEST setup implies

$$R_{c,1} = 0.8371, \quad R_{c,2} = 0.9374 \quad (9)$$

for the inner and outer vessels, respectively. The regions outside the 2σ contours will be excluded by BEST in these two cases at 95% C.L., which illustrate the BEST prospects in testing the gallium anomaly.

The plots in Fig. 3, as compared to that in Fig. 2, ensure that the status of the gallium anomaly after the BEST experiment will largely depend on its results. To support this conclusion, we calculate the joint χ^2 statistics (5) for all

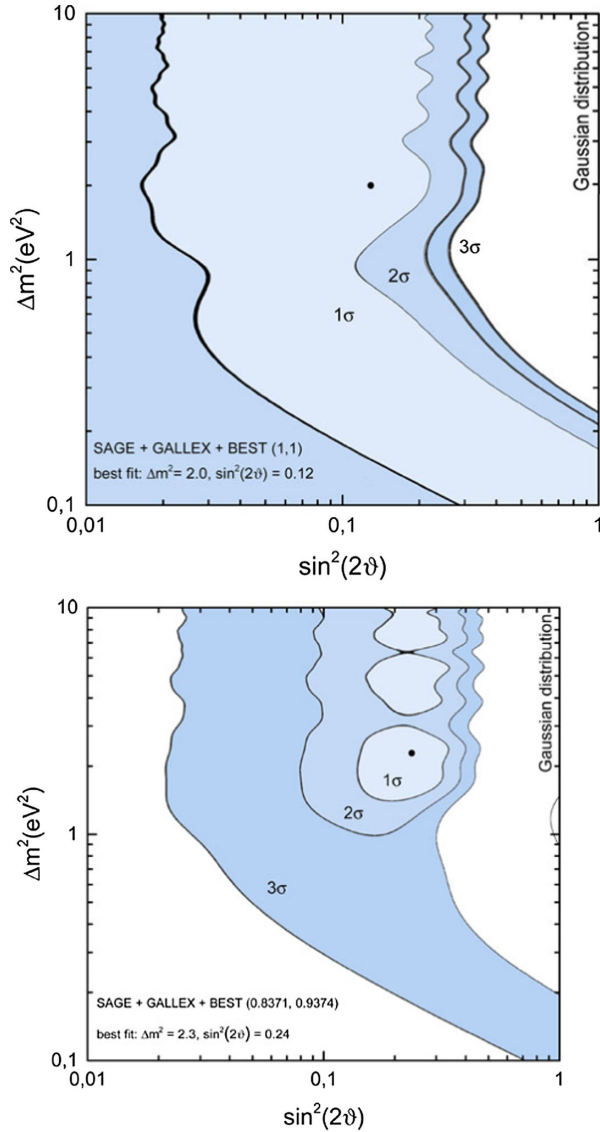


FIG. 4. Regions, favored by the combined analysis of all of the gallium radioactive source experiments in cases: (upper panel) BEST finds no anomaly, (lower panel) BEST confirms the gallium anomaly; see the main text for details.

the radioactive source experiments by SAGE, GALLEX, and BEST (six experiments in total) assuming for the latter, an error $\sigma_i = \sqrt{2}\sigma_{\text{BEST}}$ and central values R_i^{obs} consistent with either the three neutrinos only, hence $R_{c,1} = R_{c,2} = 1$, or with the best-fit values (6), and hence, ratios (9). The favored regions in these cases of the model parameter space are presented in Fig. 4.

V. CONCLUSIONS

To summarize, we present the refined estimates of BEST sensitivity to models with light sterile neutrinos mixed with electron neutrinos. We study the possible impact of the future BEST results on the status of the gallium anomaly.

The performed numerical studies are illustrated with plots in Figs. 3 and 4. It is worth noting that the region $\Delta m^2 \gtrsim 100 \text{ eV}^2$ is excluded for $\sin^2 2\theta > 0.1$ by the peak searches in β decays, the strongest limits are placed by the Troitsk ν -mass experiment [30,31]. Note also, that a sterile neutrino of mass $m_s \approx 1 \text{ eV}$ noticeably changes the cosmological prediction of the standard Λ CDM model. In particular, the Planck experiment [32] excludes masses above 0.5 eV for the fully thermalized sterile neutrino. However, this cosmological limit depends considerably on the cosmological data set used in the analysis. Also, this limit is inapplicable if the sterile neutrinos are not thermalized in the early Universe plasma of the Standard Model particles, which can happen in specific extensions of the Standard Model, see, e.g., [33,34]. Thus, cosmology still allows for the presence of light sterile neutrinos (introduced to explain the gallium anomaly) with an extended particle physics and/or cosmological model. In turn, direct searches for light sterile neutrinos, like that provided by BEST, can test such extensions.

ACKNOWLEDGMENTS

We thank F. Bezrukov, S. Demidov, and G. Rubtsov for valuable discussions. The work was supported by the RSF Grant No. 14-22-00161.

-
- [1] C. Athanassopoulos *et al.* (LSND), *Phys. Rev. Lett.* **75**, 2650 (1995).
 - [2] A. Aguilar-Arevalo *et al.* (LSND), *Phys. Rev. D* **64**, 112007 (2001).
 - [3] A. A. Aguilar-Arevalo *et al.* (MiniBooNE), *Phys. Rev. Lett.* **105**, 181801 (2010).
 - [4] A. A. Aguilar-Arevalo *et al.* (MiniBooNE), *Phys. Rev. Lett.* **110**, 161801 (2013).
 - [5] J. N. Abdurashitov *et al.* (SAGE), *Phys. Rev. C* **59**, 2246 (1999).
 - [6] J. N. Abdurashitov *et al.*, *Phys. Rev. C* **73**, 045805 (2006).
 - [7] F. Kaether, W. Hampel, G. Heusser, J. Kiko, and T. Kirsten, *Phys. Lett. B* **685**, 47 (2010).
 - [8] T. A. Mueller *et al.*, *Phys. Rev. C* **83**, 054615 (2011).
 - [9] P. Huber, *Phys. Rev. C* **84**, 024617 (2011); **85**, 029901(E) (2012).

- [10] K. A. Olive *et al.* (Particle Data Group), *Chin. Phys. C* **38**, 090001 (2014).
- [11] K. N. Abazajian *et al.*, [arXiv:1204.5379](https://arxiv.org/abs/1204.5379).
- [12] J. N. Abdurashitov *et al.* (SAGE), *Phys. Rev. C* **80**, 015807 (2009).
- [13] S. M. Bilenky, C. Giunti, and W. Grimus, *Prog. Part. Nucl. Phys.* **43**, 1 (1999).
- [14] C. Giunti and M. Laveder, *Phys. Rev. C* **83**, 065504 (2011).
- [15] C. Giunti, M. Laveder, Y. F. Li, Q. Y. Liu, and H. W. Long, *Phys. Rev. D* **86**, 113014 (2012).
- [16] V. N. Gavrin, V. V. Gorbachev, E. P. Veretenkin, and B. T. Cleveland, [arXiv:1006.2103](https://arxiv.org/abs/1006.2103).
- [17] V. N. Gavrin, V. V. Gorbachev, E. P. Veretenkin, B. T. Cleveland, S. R. Elliott, and J. S. Nico, in *Neutrino telescopes. Proceedings, 14th International Workshop, Venice, Italy, March 15–18, 2011* (Papergraf, Padova, 2011).
- [18] D. Frekers *et al.*, *Phys. Lett. B* **706**, 134 (2011).
- [19] D. Frekers *et al.*, *Phys. Lett. B* **722**, 233 (2013).
- [20] D. Frekers *et al.*, *Phys. Rev. C* **91**, 034608 (2015).
- [21] J. N. Abdurashitov, V. N. Gavrin, V. V. Gorbachev, T. V. Ibragimova, I. N. Mirmov, A. A. Shikhin, V. E. Yants, and B. T. Cleveland, *Prib. Tekh. Eksp.* **2011**, 12 (2011); [*Instrum. Exp. Tech. (USSR)* **54**, 156 (2011)].
- [22] V. V. Gorbachev, B. T. Cleveland, V. N. Gavrin, T. V. Ibragimova, A. V. Kalikhov, J. S. Nico, and E. P. Veretenkin, *J. Phys. Conf. Ser.* **375**, 042068 (2012).
- [23] V. V. Gorbachev, E. P. Veretenkin, V. N. Gavrin, S. N. Dan'shin, T. V. Ibragimova, A. V. Kalikhov, and T. V. Knodel, *Yad. Fiz.* **76**, 1591 (2013) [*Phys. At. Nucl.* **76**, 1507 (2013)].
- [24] V. N. Gavrin, *Yad. Fiz.* **76**, 1299 (2013) [*Phys. At. Nucl.* **76**, 1238 (2013)].
- [25] V. Gavrin *et al.*, *Phys. Part. Nucl.* **46**, 131 (2015).
- [26] V. V. Gorbachev, V. N. Gavrin, T. V. Ibragimova, A. V. Kalikhov, Y. M. Malyshkin, and A. A. Shikhin, *Yad. Fiz.* **5**, 892 (2014) [*Phys. Atom. Nucl.* **78**, 1617 (2015)].
- [27] E. P. Veretenkin, V. V. Gorbachev, V. N. Gavrin, S. N. Danshin, T. V. Ibragimova, Y. P. Kozlova, and I. N. Mirmov, *Yad. Fiz.* **5**, 904 (2014) [*Phys. Atom. Nucl.* **78**, 1606 (2015)].
- [28] V. V. Gorbachev and Y. M. Malyshkin, *Instrum. Exp. Tech. (USSR)* **58**, 418 (2015).
- [29] M. Cribier *et al.*, *Nucl. Instrum. Methods Phys. Res., Sect. A* **378**, 233 (1996).
- [30] A. I. Belesev, A. I. Berlev, E. V. Geraskin, A. A. Golubev, N. A. Likhovid, A. A. Nozik, V. S. Pantuev, V. I. Parfenov, and A. K. Skasyrskaya, *JETP Lett.* **97**, 67 (2013).
- [31] A. I. Belesev, A. I. Berlev, E. V. Geraskin, A. A. Golubev, N. A. Likhovid, A. A. Nozik, V. S. Pantuev, V. I. Parfenov, and A. K. Skasyrskaya, *J. Phys. G* **41**, 015001 (2014).
- [32] P. A. R. Ade *et al.* (Planck), [arXiv:1502.01589](https://arxiv.org/abs/1502.01589).
- [33] S. Hannestad, R. S. Hansen, and T. Tram, *Phys. Rev. Lett.* **112**, 031802 (2014).
- [34] B. Dasgupta and J. Kopp, *Phys. Rev. Lett.* **112**, 031803 (2014).